Follets Island: A Case of Unprecedented Change and Transition from Rollover to Subaqueous Shoals

Christopher I. Odezulu, Jorge Lorenzo-Trueba, Davin J. Wallace, and John B. Anderson

Abstract Follets Island, a transgressive island located on the upper Texas coast, is an ideal location to study barrier island transition from a rollover subaerial barrier to subaqueous shoals. This system also allows for an examination of coastal response to accelerated sea-level rise, storms, and sediment supply. The landward shoreline retreat rate during historical time is similar to the landward retreat rate of the bay shoreline, hence its current classification as a rollover barrier. However, the island has a limited and diminishing sand supply, which makes it even more vulnerable to erosion during storms and relative sea-level rise. Four core transects that extend from the upper shoreface to the back barrier bay are used to constrain the thickness of washover, barrier and upper shoreface deposits and to estimate sediment fluxes in the context of the overall sand budget for the island over centennial timescales. Stratigraphic architecture reveals two prominent transgressive surfaces. A lower flooding surface separates red fluvial-deltaic clay from overlying bay mud and an upper erosional surface separates back-barrier deposits from overlying shoreface and foreshore deposits.

Radiocarbon ages are used to constrain the evolution of the barrier and its long-term rate of island migration whereas ^{210}Pb dates are used to constrain the modern sand overwash flux. Results show that significant washover sands are deposited in the bay and about twice this volume is deposited as subaerial washover deposits. The total sand washover volume shows that overwash processes account for about half of the sand produced by shoreline erosion in historical time. Our results also indicate that the historical rate of shoreline retreat is about an order of magnitude

C.I. Odezulu (✉) • J.B. Anderson
Department of Earth Sciences, Rice University, Houston, TX, USA
e-mail: christopher.i.odezulu@rice.edu; johna@rice.edu

J. Lorenzo-Trueba
Earth and Environmental Studies, Montclair State University, Montclair, NJ, USA
e-mail: lorenzotruej@mail.montclair.edu

D.J. Wallace
Division of Marine Science, University of Southern Mississippi,
Stennis Space Center, MS, USA
e-mail: davin.wallace@usm.edu

faster than the geologic rate. We estimate back-barrier accommodation space to be about three times greater than the volume of the barrier. Hence, given the current shoreline erosion and overwash flux rate, Follets Island will eventually transition from a subaerial rollover barrier to subaqueous shoals. The frequency of severe storms along the Texas coast is not believed to have varied significantly in recent time, but the rate of sea-level rise has increased approximately five-fold and sand supply to the island is minimal. This leads us to suggest that accelerated sea-level rise and diminished sand supply are the main causes of this unprecedented change.

1 Introduction

Barrier rollover is the progressive erosion of the beach and shoreface as eroded sand is recycled and transported to the back-barrier via overwash and tidal inlet processes (Leatherman 1983; Niedoroda et al. 1985; Swift et al. 1985; Inman and Dolan 1989; Cowell et al. 2003; Stéphan et al. 2012). A barrier is assumed to maintain constant width during rollover, thereby providing stabilization during transgression (Dean and Maurmeyer 1983). However, a negative sediment budget and back-barrier accommodation space can reduce the volume of subaerial barriers during rollover processes, leading to frequent overwash and disintegration or break-up of barriers as seen in the Chandeleur Islands (Boyd and Penland 1984; McBride and Byrnes 1997; Moore et al. 2014). This process of barrier transition has wide reaching impacts because barrier islands serve as buffers to storm impacts, shielding mainland and coastal ecosystems from the full force of storm surge.

Two-thirds of the northern Gulf of Mexico coast is occupied by barrier islands (Morton et al. 2004). In Texas, 35% of barriers are progradational, 45% retrogradational, and 20% aggradational (Morton 1994). These differences reflect variable response of these barriers to relative sea-level rise and other factors since the time of their formation (Anderson et al. 2014), and this variability continues today. Historical data show that 88% of the barriers of the upper Texas coast are experiencing net shoreline retreat, but rates vary spatially and temporally along the coast (Gibeaut et al. 2000; Paine et al. 2012, 2017). Sea-level rise, limited sand supply, and storm impacts are assumed to be the main drivers of these shoreline changes (Morton et al. 2004; Wallace et al. 2009; Wallace and Anderson 2013). Sea-level and sediment supply rates control long-term shoreline changes while storms punctuate the long-term processes by shaping the morphology of barriers (Morton et al. 1995; Anderson et al. 2010, 2014; Wallace and Anderson 2013; Paine et al. 2017).

Anderson et al. (2014) suggest that modern rates of shoreline retreat along the upper Texas coast are unprecedented, arguing that the current shoreline would be

located kilometers inland of its current location if these rates had occurred since these barriers first began migrating landward. For example, Galveston Island formed ~5.5 ka and experienced an extended period of progradation that ended around 1.8 ka (Bernard et al. 1959, 1970; Rodriguez et al. 2004). Today, the west end of the island, which is not protected by a seawall, is retreating at short-term rates between 1.4 and 3.9 m/year (Paine et al. 2012). If the long-term landward retreat rate since 1.8 ka was the same as the current average rate, the shoreline would be located about 4.7 km landward of its current location. By determining the sequestration location of eroded material from Galveston Island beaches and nearshore environments through time, Wallace and Anderson (2013) were able to quantify short-term and long-term volumetric erosion. Consistent with observations elsewhere by FitzGerald et al. (this volume), Wallace and Anderson (2013) demonstrated that unprecedented historic erosion of Galveston Island is supported by accelerated growth of the San Luis Pass tidal delta in historical time, as this tidal delta is the ultimate sink for most of the sand eroded from the island. They further argued that this unprecedented change was due to accelerated sea-level rise punctuated by storm events.

South Padre Island is an even more dramatic case of unprecedented shoreline retreat in modern time. Distal overwash deposits in Laguna Madre and barrier island sands date back to ~4 ka, indicating that the island has not moved significantly during the late Holocene (Wallace and Anderson 2010), while the current rate of shoreline retreat of ~1.90 m/year would have resulted in ~7.6 km of retreat over this time interval.

Follets Island is a relatively small barrier located west of Galveston Island (Fig. 1). It is classified as a low-gradient retrogradational barrier in a rollover phase, based on sediment cores that have sampled back-barrier deposits below modern barrier and shoreface deposits (Bernard et al. 1970; Morton 1994; Wallace et al. 2010; Anderson et al. 2014). Indeed, it is one of the fastest retreating barriers of the Texas coast. The historical shoreline retreat rate averages ~2.0 m/year (Morton 1994; Gibeaut et al. 2000; Paine et al. 2012).

Though the causes of Follets Island's historic shoreline retreat are known to be both natural (limited sand supply, relative sea-level rise, and storm impacts) and anthropogenic (diversion of the Brazos River mouth and construction of jetties at the old river mouth), the impact of each factor alone has not been quantified. Numerical modeling is needed to evaluate the individual contributions of these agents to current shoreline retreat and to predict future changes to the island. But, quantitative prediction of the island's response to sea-level rise and storms is difficult due to the complex nature of these processes and stochastic storm frequency. To gain further insight, detailed stratigraphic resolution is needed to match specific events with historical records. In addition, the high-resolution, short-term sand budget of the island must be determined; specifically the amount of sand being transported offshore and backshore versus the amount of sand moving within the longshore transport system. Furthermore, the thickness of barrier sands must be determined to quantify the rate of sand generated by erosion and cannibalization of the island.

Fig. 1 Location of Follets Island and nearby coastal features. Study area (Fig. 3) shown by *red box*

Here, our objectives are (1) to determine the thickness of sand composing Follets Island and the adjacent shoreface, (2) to determine the modern overwash flux for the island as it relates to the volume of sand that has been eroded from the island during historical time, (3) to compare current rates of shoreline erosion to the geological rate in order to assess the magnitude of change over time, (4) to determine if and when Follets Island will transition from a rollover subaerial barrier to subaqueous shoals, and (5) to describe the response of the island to external forcings and predict the island's future.

2   Study Area

Follets Island is a long (10 km), narrow (average 350 m), low-lying (<2 m high, excluding artificial dunes) barrier bounded by the Gulf of Mexico to the south and Christmas Bay to the north (Fig. 1). It is a diurnal, micro-tidal (less than 0.5 m tidal amplitude), wave-dominated environment (Morton et al. 2004). Southeasterly winds are prevalent most of the year, with prevailing longshore currents toward the west. During winter, cold fronts result in a reversal in longshore currents, from west to east (Morton et al. 1995).

The average rate of long-term subsidence for the upper Texas coast is low, averaging ~0.05 mm/year (Paine 1993). However, this rate varies along the coast due to compaction of Holocene sediments, which vary in thickness from <1 to 50 m, a reflection of the relief on the Pleistocene surface that underlies the coast (Anderson et al. 2014). Follets Island is situated above the eastern margin of the Brazos River incised river valley and is flanked on its eastern and western sides by Holocene Brazos River channels belts; the Bastrop Channel belt and Oyster Creek channel belt, respectively (Bernard et al. 1959; Morton 1994; Rodriguez et al. 2004; Wallace et al. 2010). Drill cores and shallow seismic data indicate an average thickness of Holocene fluvial sediments of ~10 m beneath the island (Bernard et al. 1970; Taha and Anderson 2008; unpublished data). So, the rate of subsidence related to compaction of these Holocene sediments is contributing to the overall relative sea-level rise in the area and is believed to be higher than the average regional rate.

Sand is supplied to Follets Island mainly through episodic recycling of the San Luis Pass tidal inlet, located just east of the island (Morton et al. 1995) (Figs. 1 and 2). During the past three decades, the island has experienced high rates of erosion (Fig. 2a) indicating that sand delivery from the tidal inlet through alongshore transport (westward) is providing negligible amounts of sand to maintain the island. Sand supply from the west has been decreased by diversion of the Brazos River mouth to the west of its pre-1929 location and construction of jetties at the former river mouth at Surfside, Texas (Morton and Pieper 1975) (Fig. 2b).

3 Methodology

Thirty-four vibracores, between 100 and 520 cm in length, and 40 surface samples were collected along four transects extending from the upper shoreface across the barrier and Christmas Bay (Fig. 3). Immediately after acquisition the cores were split, photographed, and described for lithology, macrofossil content, and sedimentary structures. Grain size analyses were conducted using a Malvern Mastersizer 2000. This instrument utilizes laser diffraction in sediment suspended in water to obtain measurements. All 34 vibracores were sampled for grain size analysis. The sampling interval depended on the core length and objective of the analysis. Most cores from Christmas Bay and the upper shoreface were sampled at 10 cm intervals to determine sand fluxes through time as a function of distance from the barrier. Cores from the beach and subaerial part of the barrier were sampled at targeted intervals to help distinguish facies.

LiDAR was used to map the barrier topography and backshore water depths. Carlin et al. (2015) conducted a detailed side-scan sonar and CHIRP survey offshore of Follets Island and their data were used for establishing the offshore profile and sub-bottom geology.

A total of 21 macrofossils were radiocarbon dated from 14 cores (Fig. 3; Table 1) using the continuous flow gas bench accelerator mass spectrometer method at the Woods Hole Oceanographic Institution (NOSAMS). Where possible, we used
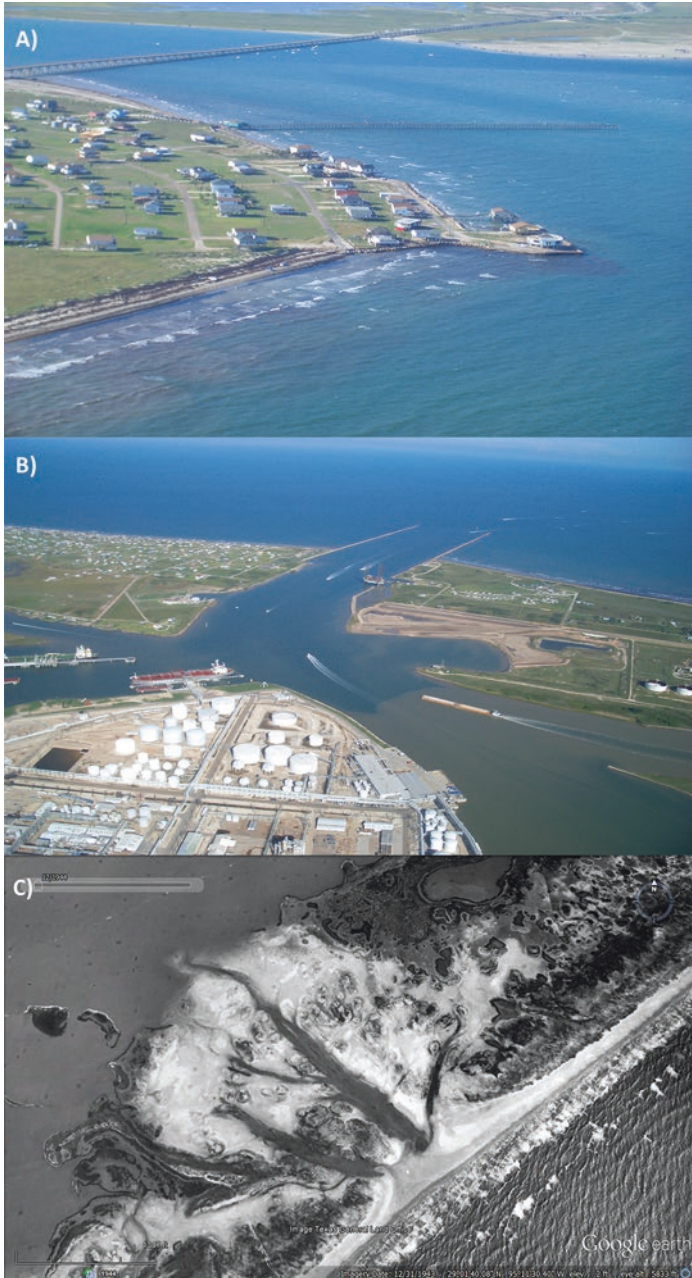
Fig. 2 (**a**) Photo showing beach erosion at the east end of Follets Island. The houses located on the spit of land protruding into the Gulf were previously located behind a dune line. (**b**) Photo facing south showing Freeport jetties, which block longshore transport of sand from the west and the Brazos River. (**c**) Breach in the island and overwash that resulted from an unnamed storm event in December 1944
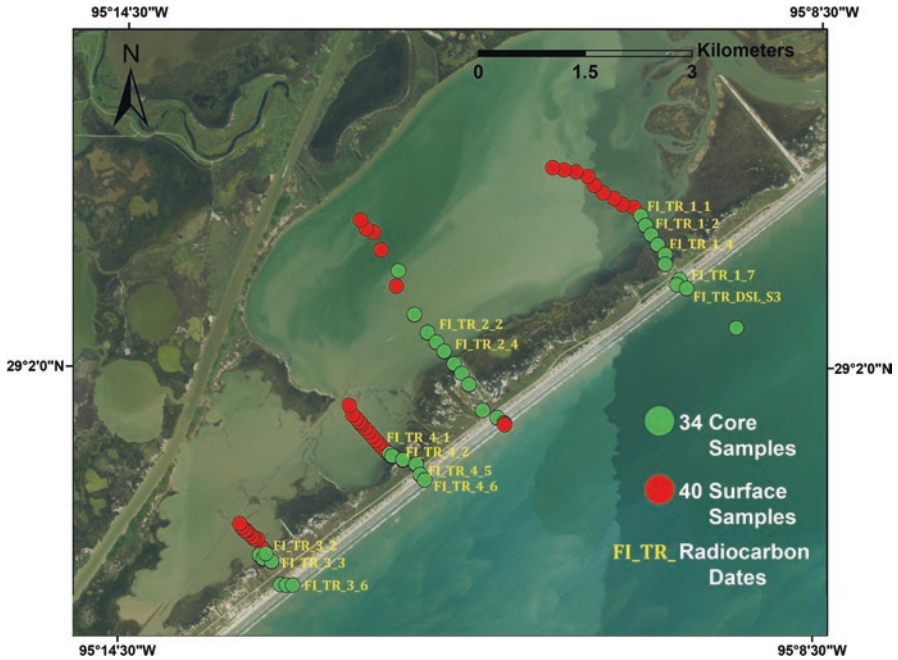
Fig. 3 Locations of sediment cores (*green circles*), cores sampled for radiocarbon dating (*yellow letters*), and surface samples (*red circles*) used for this study

articulated *Rangia cuneata* and *Ensis directus* (Razor clams), indicating largely in situ samples (Fig. 4). Table 1 provides details of the radiocarbon analyses. Radiocarbon ages were reported as calibrated years before present (where present is CE 1950). Using the standard 400-year marine reservoir correction, the ^{14}C ages were converted to calibrated calendar years at the 95.5% confidence interval (2 sigma ranges) with Marine 13 using the CALIB.Rev. 5.0 program (Reimer et al. 2013).

In addition to radiocarbon dating, ^{210}Pb analysis was conducted on cores 2-4 and 4-1 to constrain the age of modern overwash deposits (Fig. 5). The top 14 cm and 21 cm of core 2-4 and 4-1, respectively, were sampled for ^{210}Pb activity. The two cores were collected using a short transparent plastic tube. The samples were carefully cut on site immediately after extrusion to avoid mixing at the sediment–water interface. Core 2-4 was sampled entirely at a 2 cm interval whereas Core 4-1 was sampled at a 2 cm interval for the first 10 cm and at a 4 cm interval for the remaining 11 cm of the extruded core. Samples were analyzed at Core Scientific International. With a half-life of 22.3 years, ^{210}Pb can effectively date sediments younger than ~150 years (Faure 1986). Constant Rate of Sedimentation (CRS) and Constant Initial Concentration (CIC) are two major models for ^{210}Pb analysis, but CRS is the most widely used (Appleby 1998). It is a reliable method for calculating ^{210}Pb ages when the rate of sediment accumulation is not constant (Appleby and Oldfield 1983). Independent validation of the chronology is necessary for a high level of confidence in the result. We could not conduct ^{137}Cs and ^{241}Am to validate the ages

Table 1 Radiocarbon ages from cores used for this study

Core ID	Material	Depth (cm)	Age Uncalibrated 14C years BP	±	2 Sigma start (BP) Calibrated 14C years BP	2 Sigma end (BP) Calibrated 14C years BP
FI_TR_2-4	*Rangia cuneata* fragment	50	530	172	0	448
FI_TR_4-1	*Ensis directus*	90	496	173	0	431
FI_TR_1-1	*Chione elevata*	130	945	175	241	894
FI_TR_DSL_S3	*Rangia cuneata*	300	3160	177	2527	3403
ªFI_TR_1-2	*Argopectin irradians*	190	1665	174	856	1595
FI_TR_1-7	*Perna perna*	260	2540	180	1804	2691
FI_TR_3-3	*Rangia cuneata*	115	507	173	0	436
ªFI_TR_5-1	Articulated *Ensis directus*	290	1330	176	565	1238
FI_TR_1-2	*Ensis directus* fragment	160	1436	177	652	1315
FI_TR_3-3	*Rangia cuneata*	170	1794	182	960	1754
ªFI_TR_3-6	*Crassostrea virginica*	265	4228	181	3854	4806
FI_TR_4-6	*Ensis directus* fragment	205	2355	176	1543	2401
FI_TR_2-2	Articulated *Rangia cuneata*	265	3734	179	3222	4144
FI_TR_3-6	*Rangia cuneata*	360	3724	183	3201	4144
ªFI_TR_5-2	*Crassostrea virginica*	250	1783	175	958	1719
FI_TR_1-4	*Ensis directus* fragment	165	1619	175	795	1526
ªFI_TR_1-6	*Perna perna*	145	3286	179	2723	3545
FI_TR_3-2	*Ensis directus* fragment	100	504	173	0	435
FI_TR_4-1	*Crassostrea virginica*	100	1028	176	292	929
FI_TR_4-5	*Rangia cuneata*	300	3724	189	3179	4157
FI_TR_4-2	Articulated *Ensis directus*	90	542	179	0	462

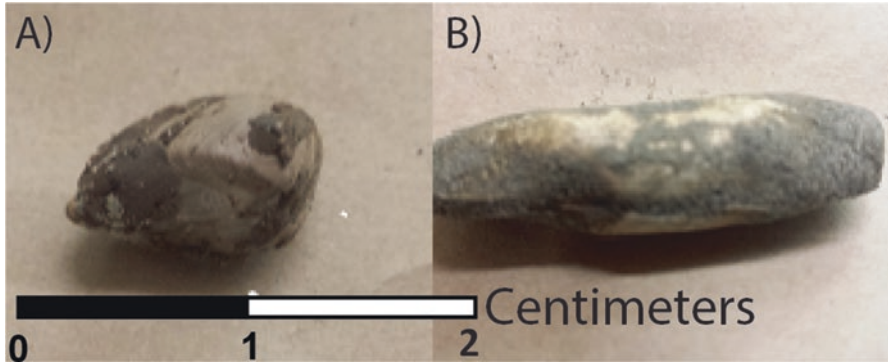ªRejected due to unlikely age-depth relationship

Fig. 4 (**a**) Photo showing Articulated *Rangia cuneata* and (**b**) *Ensis directus* clams targeted for radiocarbon dating

but we compared results from both CRS and CIC models for more accurate estimates. It is assumed that ^{210}Pb activity of lakes and bays has a supported component that was generated in situ within the sediment column, and the unsupported component came from the atmosphere (Appleby 1998) (Fig. 5).

4 Results

4.1 Lithofacies

Lithologic logs for sediment cores collected along four transects are shown in Fig. 6. Based on modern distribution patterns and visual descriptions of cores augmented by grain size data (Fig. 7), lithofacies were differentiated into upper shoreface sand, beach sand, proximal and distal washover deposits, bay mud, and fluvial/ delta plain red clay (Fig. 8a–d). A brief description of these lithofacies follows:

Upper shoreface sands are fine (120–150 μm), well-sorted, with abundant shell debris and rare stratification (Fig. 8a).

Beach sands consist of well-sorted, yellowish-brown, structureless, fine sand (140–200 μm). Shells are common, including shell lags up to 10 cm thick (Fig. 8c, d).

The proximal overwash environment is a subaerial zone that occurs just bayward of aeolian dunes, which are mostly less than 2 m in elevation. The overwash zone is marked by a change to relatively flat relief and includes much of the back-barrier intertidal zone. The lithofacies consists dominantly (>90%) of very fine to fine (size range from 70 to 190 μm), moderately to well-sorted sand, with root casts and a virtual absence of shells (Fig. 8b, c).

The distal overwash facies is a subaqueous facies that extends bayward from the bay shoreline to where overwash transitions into bay mud. It is a poorly sorted, muddy-sand/sandy-mud and ranges in color from brown to gray. It is burrowed and
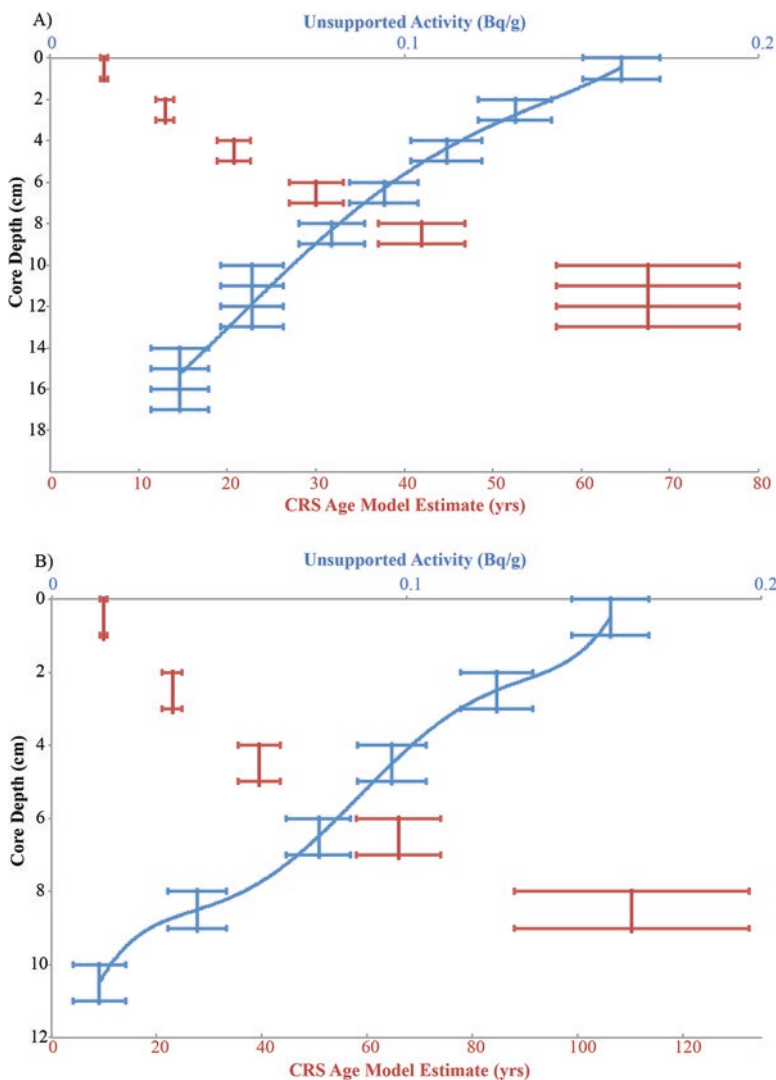
Fig. 5 Plot showing unsupported ^{210}Pb decreasing with depth for cores 4-1 (**a**) and 2-4 (**b**). Plotted are the unsupported ^{210}Pb activity (Bq/g) represented by *blue* and the CRS age model estimate (years) represented by *red* for both sample range depths

characterized by isolated shells, mainly *Rangia cuneata*, *Ensis directus* (razor clams), *Chione elevate*, and *Argopecten irradians* (scallop) (Fig. 8b, c). Results from grain size analyses show that it is a mixture of very fine sand and coarse silt (40–120 µm, Fig. 7).

Bay mud is a gray to dark gray mixture of sand and mud, which includes more fine silt and clay than the distal overwash facies (Fig. 8b). This facies is characterized by abundant shells; most abundant are *Crassostrea virginica* (oysters) and *Rangia cuneata*.
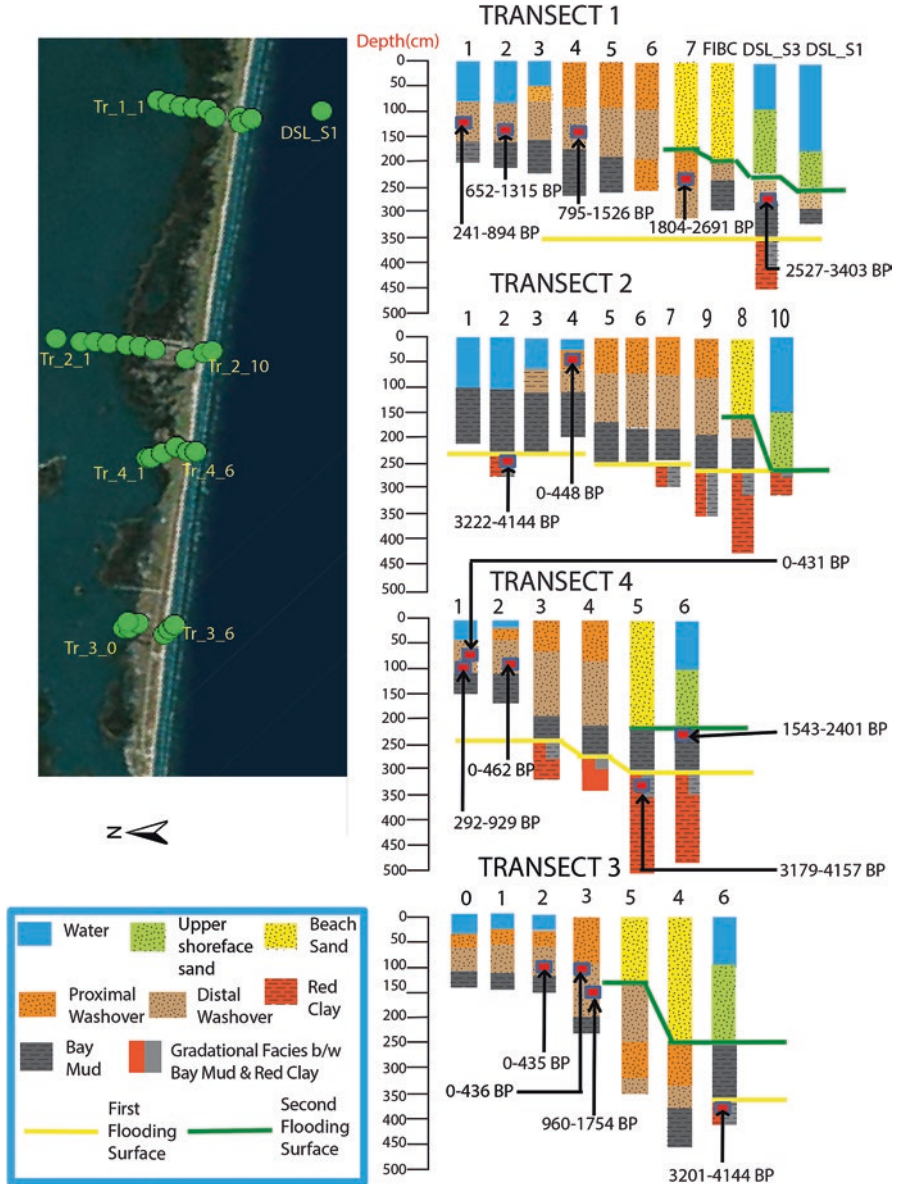
Fig. 6 Core locations and lithologic logs. Also shown are 2 sigma radiocarbon age ranges. Two flooding surfaces are identified. The younger (*green*) surface separates modern beach and foreshore sands from underlying back-barrier overwash deposits and bay mud. An older (*yellow*) surface is the initial bay shoreline flooding surface and separates bay mud from underlying fluvial and delta plain deposits

Fig. 7 Sorting versus mean grain size data for samples from different lithofacies
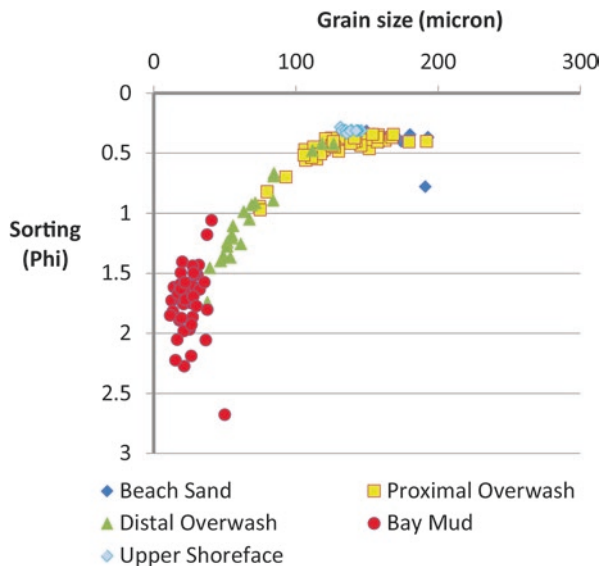
The oldest facies consists of compacted red clay that is mostly barren of fossils and root casts (Fig. 8a). This is a flood plain-delta plain facies associated with the ancestral Brazos River, which occupied channels on either end of Follets Island during the late Holocene (Bernard et al. 1970).

4.2 Stratigraphy

CHIRP profiles collected offshore of Follets Island by Carlin et al. (2015) show a thin upper shoreface unit resting on older strata. Our sediment cores from the upper shoreface sampled a thin (less than ~1.5 m thick) sand unit resting above the red fluvial-deltaic clay, bay, and washover lithofacies (Fig. 6). Radiocarbon ages from cores indicate that the red clay is older than ~4.1 ka, which is consistent with radiocarbon ages obtained onshore from Brazos paleo-channel deposits (Bernard et al. 1970).

The red clay unit is overlain by, and in sharp contact with, bay mud. This contact is the bay shoreline flooding surface, which represents initial flooding and creation of Christmas Bay. Radiocarbon ages from cores 2-2, 3-6 and 4-5 indicate initial bay flooding began between approximately 4.2 and 3.2 ka (Fig. 6; Table 1), which is consistent with the sea-level record for the northwestern Gulf of Mexico (Milliken et al. 2008).

Cores through Follets Island penetrated between ~2.0 and 2.5 m of beach sand. Beneath the barrier sand, cores sampled back-barrier washover and bay deposits (Fig. 6). Cores from the subaerial back-barrier zone sampled proximal washover
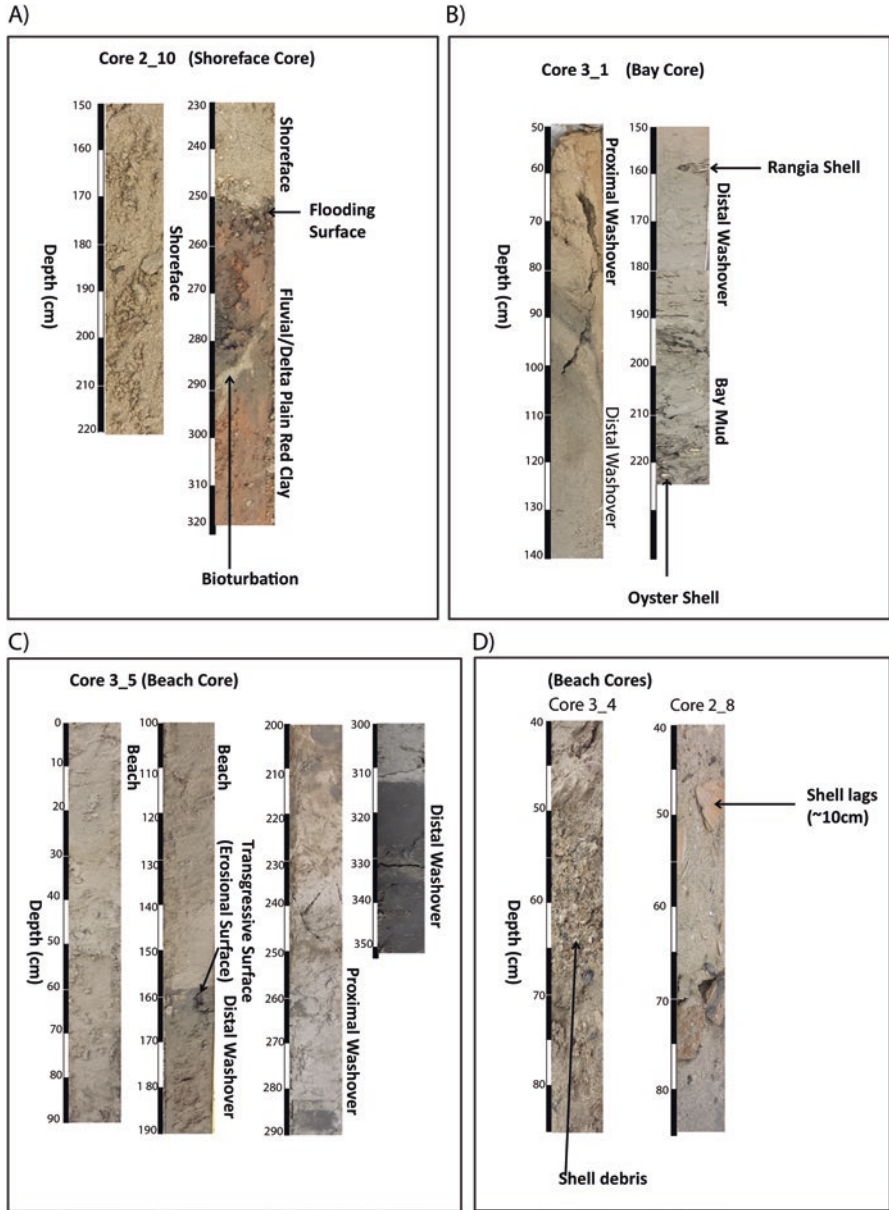
Fig. 8 Core photos of (**a**) shoreface facies, (**b**) bay facies, (**c**) and (**d**) beach facies sampled in sediment cores

deposits resting in sharp contact on distal washover deposits, which rest on, and have a gradational contact with, bay muds (Fig. 8b, c).

The observed stratigraphic architecture recorded by our sediment cores reveals two prominent transgressive surfaces. The lower surface occurs at a depth of between ~2.5 and 4 m (yellow line in Fig. 6) and separates red clay (Holocene delta plain and flood plain deposits of the Brazos River) from overlying bay mud. The contact between these units is gradational, indicating little or no erosion. The upper transgressive surface is a planar, sharp surface at a depth between ~1.5 and ~3 m (green line in Fig. 6) separating back-barrier sediments from overlying upper shoreface and/or beach deposits.

The Transgressive Ravinement Surface (TRS) occurs at an average depth between 8 and 12 m along the upper Texas coast (Siringan and Anderson 1994; Rodriguez et al. 2001; Wallace et al. 2010). We did not sample this surface, but CHIRP profiles from offshore Follets Island show that at approximately −8 m marine muds onlap older Pleistocene and Holocene deposits (Carlin et al. 2015).

Thin upper shoreface sands off Follets Island are unique in the context of the Texas coast. Offshore Follets, sand thicknesses are only ~1 m thick compared to at least 5 m thick upper shoreface sands for other Texas barriers (Siringan and Anderson 1994; Rodriguez et al. 2001; Wallace et al. 2010). This suggests that the Follets Island shoreface is starved of sand, which is supported by grain size data. Upper shoreface sands are notably finer than beach sands, indicating minimal offshore sand transport of beach material (Fig. 7).

4.3   Sand Budget and Flux Analysis

To predict future changes to Follets Island accurately, the sand budget of the island must be determined. Sand budgets can be used to investigate the overwash flux of sediments eroded from the shoreface (Inman and Dolan 1989), and to understand the dynamics of sand sources and sinks for a barrier environment. Precise sand budget analyses involve well-constrained sand volumes. Most published data on washover sediment budgets are derived from field measurements and aerial photographs to quantify washover. Specifically, washover penetration distances and thicknesses determined for modern events (Morton and Paine 1985; Morton and Sallenger 2003) or time series of beach profiles (Park and Edge 2011) form the basis for conclusions when there is little sediment core chronology available. The greatest uncertainty in deriving washover fluxes using these methods arises from the limited information on unit thickness and age. Good core coverage and improved chronostratigraphic resolution, coupled with information gained from aerial photographs and detailed topographic data, have provided sufficient detail to relate pre-historic and historic overwash rates (Donnelly et al. 2006; Carruthers et al. 2013; Rodriguez et al. this volume). The results from these later studies provided motivation for our work.

4.3.1 Sand Overwash Estimate

Long-term, millennially averaged sand fluxes have been quantified for Follets Island over the past ~3000 years (Wallace et al. 2010). These longer-term values can help put the historic values into context and allow for a better understanding of short-term coastal morphologic change.

We can constrain modern accumulation rates for distal overwash using ^{210}Pb (Fig. 5a, b). For core 4-1, the measured unsupported activities for the topmost 17 cm of the core range from 0.161 to 0.037 Bq/g (Fig. 5a). Measured unsupported activity (Bq/g) values in the uppermost 11 cm of core 2-4 range from 0.157 to 0.013 Bq/g (Fig. 5b). The accumulation rate was calculated using the constant rate of supply (CRS) model of Appleby and Oldfield (1983), which assumes a constant flux of unsupported ^{210}Pb but varying rate of sediment accumulation over time. From the age model, the oldest reliable associated age for core 2-4 of ~70 years occurs as shallow as 6 cm (using the shallowest depth interval), and this same age occurs in core 4-1 as deep as 13 cm (using the deepest depth interval). Therefore, the maximum spread of calculated sedimentation/accumulation rates from the ^{210}Pb results range between ~0.86 and 1.86 mm/year (6–13 cm/~70 years).

To determine the volume of modern sand overwash, we first estimated the thickness and extent of proximal overwash deposits using aerial photographs and sediment cores. The average total thickness of proximal overwash sand varies between transects from 1.5 m to a few decimeters and decreases bayward (Fig. 6). The area of the proximal overwash was estimated to be 3,500,000 m^2 (10 km length by 350 m width). We determined a 0.19 m thickness for modern overwash based on the assumption that proximal overwash is twice the highest average value from the distal overwash for the last ~70 years (thickness of distal overwash estimated from ^{210}Pb is between 6–13 cm for the last ~70 years). This is likely a minimum value based on the observation of rapid thinning of modern overwash deposits at the bay shoreline, the approximate boundary between proximal and distal overwash deposits. Based on this analysis, we estimate the modern proximal overwash sand volume to be ~665,000 m^3 (3,500,000 m^2 × 0.19 m).

The next step was to measure the concentration of 100–200 μm sand within distal washover and bay sediments in the tops of the cores and in grab samples. This size range encompasses the sand that comprises Follets Island and its shoreface (Fig. 7). Our radiocarbon dates differentiate the overwash deposits into modern (<500 years), intermediate (~1200 years), and paleo overwash (between ~2000 and ~3700 years) units (Fig. 9). The long-term accumulation rate is roughly linear at ~1.0 mm/year.

We measured the volume of sand in modern distal washover and bay sediments using core tops and grab samples. As expected, the concentrations decrease with increasing distance from the bay shoreline (Fig. 10). A surprising outcome of this analysis is that 20–30% sand (between 100 and 200 μm) comprises Christmas Bay sediments for distances of up to 1.5 and 2.3 km from the bay shoreline in transects 1 and 2, respectively. Note that surface samples collected more than 1.5 km from the bay shoreline along transect 1 contain ~25% sand. We attribute these relatively high

Fig. 9 Radiocarbon age clusters are used to subdivide washover deposits into units by age: modern (<500 years), intermediate (average 1200 years), and paleo washover (between ~2000 and 3700 years)
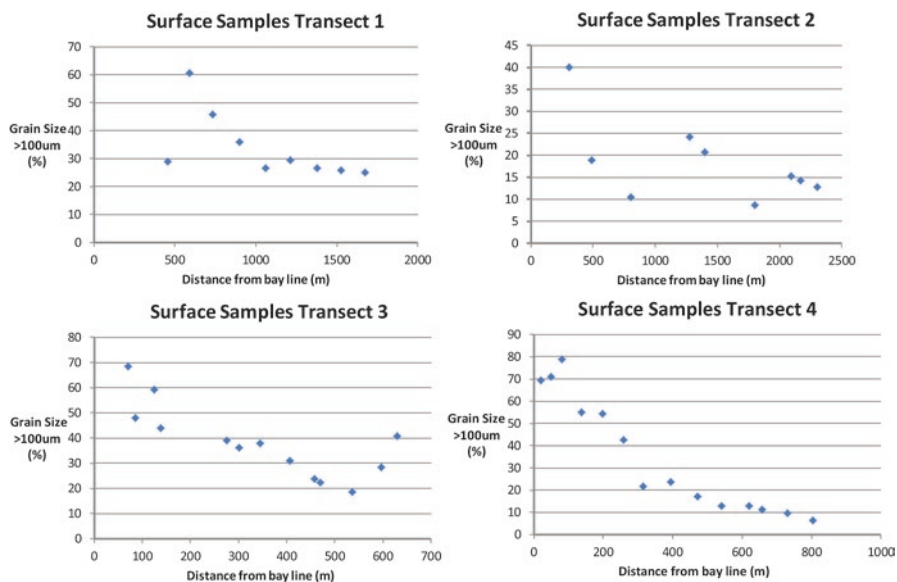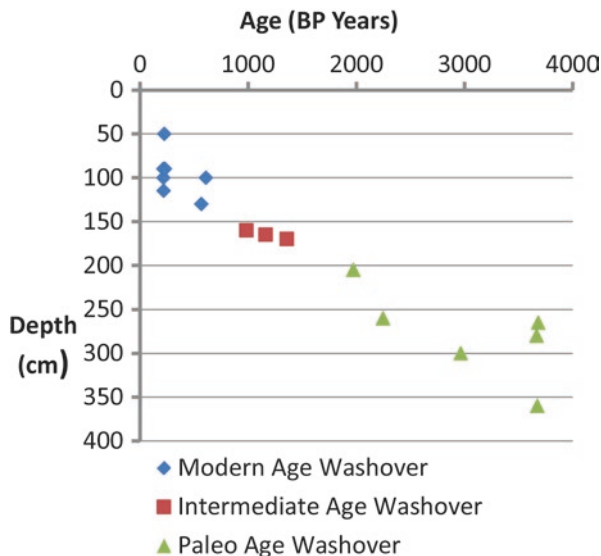

Fig. 10 Sand (100–200 μm) concentration, representing lower limit of sand concentration that makes up Follets Island and the shoreface, with increasing distance (northward and into Christmas Bay) from the bay shoreline (bay line) for each sample transect

concentrations to the proximity of the San Luis Pass tidal delta within the eastern part of Christmas Bay (Fig. 3). Transects 3 and 4 also show the expected decrease in sand volume with distance from the bay shoreline, but the distances are less than in transects 1 and 2. Note that transect 3 shows a decrease and then an increase in sand with distance from the bay shoreline. This increase is attributed to the close proximity of a dredge spoil area where sand concentrations increase. These samples were not included in our overwash sand flux calculations. The difference in transport distance between transects 1 and 2 versus transect 3 and 4 is attributed to the shallower water depths of transects 3 and 4. We made grids that range from 950,000 to 1,175,000 m^2 in areal extent (500 m length, distance interval from the bay shoreline, and the distance between two transects) and then multiplied by the sand (100–200 μm) concentration in the grid (Fig. 11). Based on this analysis, we estimate the modern distal overwash sand flux into Christmas Bay to be ~399,000 m^3 (10 km barrier length by average of 420 m width and 0.095 m average overwash thickness for the last ~70 years). The 0.095 m thickness was the average of 0.13 m and 0.06 m, the maximum and minimum overwash flux in 70 years for cores 4-1 and 2-4 respectively. Again, the modern proximal overwash sand volume is ~665,000 m^3 (0.95 m^3/m/year), which yields a total modern overwash volume of ~1,064,000 m^3 for the last ~70 years (1.52 m^3/m/year). Flux units are presented as m^3/m/year (average flux per meter of shoreline) and m^3/year (total volumetric accumulation).

The next step is to see how this total modern overwash volume compares with the total volume of sand eroded from the island in historical time. A key assumption is that the total thickness of sediment eroded is ~1.5 m. The 1.5 m thickness used is the average of proximal overwash, beach, and upper shoreface sands sampled in cores. Though the ravinement surface is about 8–10 m water depth, the acoustic back scatter from the CHIRP data shows that there is no sand below ~4 m water depth (Carlin et al. 2015).

Using these values, we are able to relate the total volume of ~2,100,000 m^3 (3.0 m^3/m/year) sand eroded (2.0 m/year modern erosion rate × 10,000 m length × 1.5 m thickness × 70 years) from the shoreface and beach over the period of observation (70 years) with the overwash volume. (The calculation of sand eroded neglects erosion of the bay sediments outcropping on the shoreface because grain size analysis indicates sand content is negligible in this facies where it outcrops on the shoreface.) Total modern sand overwash volume is ~1,064,000 m^3 (1.52 m^3/m/year) for the same time interval, suggesting that a little over half of the sand eroded from Follets Island in recent decades can be accounted for in the sand overwash estimates.
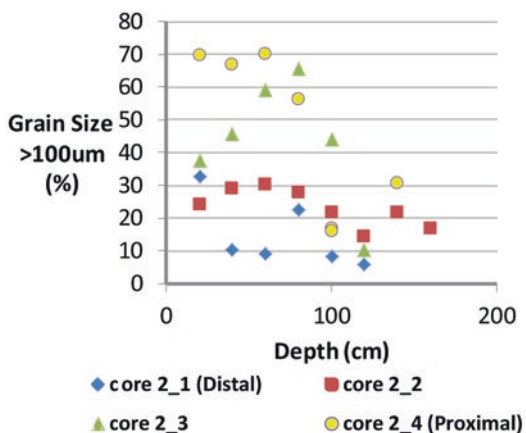
4.3.2   Drowning Time Estimate

Based on the flux of sand eroded from the foreshore and shoreface (3.0 m^3/m/year) and the total overwash flux (1.52 m^3/m/year), we estimate that the sand volume of Follets Island has been reduced at a rate of 1.48 m^3/m/year over the past 70 years.

Fig. 11 Sand (100–
200 μm) concentration
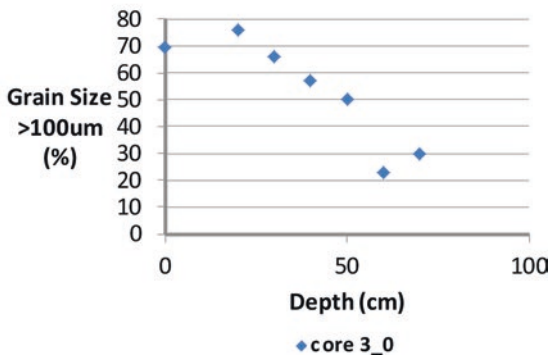trends with depth in cores
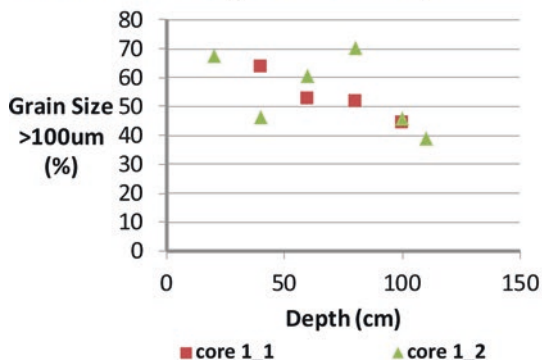
Additionally, we note that a significant fraction of the total overwash flux is deposited into Christmas Bay, far from the back-barrier shoreline, where it cannot contribute to maintaining the sand volume of Follets Island in the near future. In particular, assuming that only the proximal overwash flux (0.95 m³/m/year) contributes to the landward migration of Follets Island, the future rate of sand loss will be 2.05 m³/m/year. At this rate, and given that the volume of Follets Island is 525 m³/m (350 m width × 1.5 m thick), we estimate the time of drowning to be ~260 years.

We consider 260 years an upper limit estimate because it does not incorporate the effect of future sea-level rise rates or future barrier narrowing, which can potentially result in a significant increase in sand flux to Christmas Bay. Future numerical modeling efforts will explore these effects.

4.3.3   Modern Versus Long-Term Overwash Flux

Cores collected within the upper shoreface to beach zones along transects 1, 2, and 3 sampled beach and shoreface sands resting unconformably on paleo overwash and bay deposits (Fig. 6). Cores DSL S3 (Transect 1) yielded a two-sigma calibrated ¹⁴C age range of 2527 to 3403 and core 1-7 yielded a two-sigma calibrated ¹⁴C age range of 1804 to 2691 BP for these deposits (Fig. 6). Thus, the current island location was a back-barrier bay during this time interval. There is a cluster of radiocarbon ages from mostly paleo overwash deposits at ~3 ka (Fig. 9), which supports the previously known age of the barrier (Wallace et al. 2010). The modern proximal overwash occurs between 500 and 800 m from the present-day Gulf of Mexico shoreline. This implies that the barrier was within 500–800 m of its current location around 3 ka. Based on these distances and ages, we estimate the long-term rate of shoreline retreat of the barrier to be in the range of 0.17–0.27 m/year (500–800 m over 3 ka), compared to a modern measured rate of 2.0 m/year, or about an order of magnitude difference.

We attempted to independently constrain the pre-modern rate of bay shoreline retreat (landward movement of the bay shoreline) by examining down-core sand concentrations (100–200 μm) as compared to the concentrations of sand in surface sediments from Christmas Bay (Fig. 10). Cores collected nearest the bay shoreline (e.g. core 3-0) show a clear decrease with depth while the cores distal to the bay shoreline show less variability with depth, probably due to bioturbation. Whereas most cores show a decrease in sand concentration with depth, there is no clear trend that allows us to estimate bay shoreline retreat rates through time from these data.

4.3.4   Back-Barrier Accommodation

Christmas Bay has an areal extent of ~27,000,000 m² and an average depth of 1.5 m. Thus, the bay has a total accommodation of 40,500,000 m³.

5   Discussion

The rate of shoreline retreat for Follets Island is nearly equal to the rate of bay shoreline retreat as measured by the Bureau of Economic Geology (Morton et al. 2004; Paine et al. 2012). Our data show exposure of back-barrier sediments in the shoreface. Our results also show that the washover accumulation rate accounts for a little over half the volume of sand estimated from the shoreline erosion rate.

Cores that penetrated Follets Island reveal that the sand that composes the island is less than 2 m thick (similar to Onslow Beach discussed in Rodriguez et al. this volume). Compared to other Texas barriers (Bernard et al. 1959; Morton and Amdurer 1974; Wilkinson 1975; Wilkinson and Basse 1978; Rodriguez et al. 2001; Simms et al. 2006; Wallace and Anderson 2010; Anderson et al. 2014), it is the thinnest barrier island on the Texas coast. Likewise, cores from the upper shoreface sampled no more than 1.5 m of sand and CHIRP profiles indicate very thin to no lower shoreface deposits below approximately 4 m water depth (Carlin et al. 2015). This is in stark contrast to other portions of the Texas coast where shoreface deposits are thicker and extend to the toe of the shoreface between approximately 8 and 12 m water depth (Siringan and Anderson 1994; Rodriguez et al. 2004). These observations suggest that the barrier has been sand-starved in historical time.

Sediment cores sampled two transgressive surfaces, a flooding surface (lower) and an erosional shoreface surface (upper). The upper surface places beach facies and upper shoreface deposits on top of back-barrier and fluvial-deltaic deposits. Both surfaces occur above the level of transgressive ravinement for the upper Texas coast, which is at about −8 m in this area (Siringan and Anderson 1994; Rodriguez et al. 2001; Wallace et al. 2010). The Transgressive Ravinement Surface (TRS) generally coincides with the toe of the shoreface and is marked by marine mud that onlaps Pleistocene deposits. The depth of the TRS indicates that it is coincident with storm wave base (Wallace et al. 2010).

Most models for shoreface and shoreline retreat rely on transgressive ravinement and assume an equilibrium shoreface configuration to account for translation (e.g. Bruun 1954, 1962; Swift 1976; Thieler et al. 2000). These models are applicable to Galveston Island and Mustang Island, where offshore core coverage allows detailed stratigraphic analysis (Siringan and Anderson 1994; Rodriguez et al. 2004; Wallace et al. 2010). But, in the case of Follets Island, the shoreface ravinement surface shows a decoupling between the upper and lower shoreface, and a coupling between upper shoreface and back-barrier (e.g., Stive and de Vriend 1995; Cowell et al. 2003). The equilibrium shoreface profile assumption does not hold in this case, at least over short timescales (i.e., the shoreface might be out-of equilibrium: Moore et al. 2010; Lorenzo-Trueba and Ashton 2014). Sediments from the upper shoreface are reworked landwards, exposing back-barrier deposits buried only by a thin veneer of upper shoreface and beach sand. This is consistent with observations of Carlin et al. (2015), who examined beach and offshore profiles collected before and after Hurricane Ike, which made landfall in 2008 approximately 20 km east of Follets Island but breached the island in 75 places (Harter et al. 2015). They noted little

change in the lower shoreface profile but a shift in the profile of the upper shoreface and beach that indicates landward movement of sand. This is consistent with the rollover process. Shell debris and shell lags are ubiquitous in cores collected from the upper surface, and record episodes of storm erosion (Fig. 8). The reason for the shallowness (~2 m) of this surface remains uncertain.

The millennial timescale overwash flux for Follets Island is about 2300 m^3/year (~0.23 m^3/m/year) (Wallace et al. 2010). Compared to the current rate of ~15,200 m^3/year (1.52 m^3/m/year), the historical rate is about an order of magnitude faster than the long-term rate. In addition, grain size analyses of the bay sediment qualitatively indicate that distal overwash fluxes have been much higher recently than they were on the millennial timescale; sand content in the present bay sediment is significant, while it is negligible where the bay sediment outcrops on the shoreface. Our estimates of total overwash volume deposited in ~70 years is ~1,064,000 m^3 (overwash flux ~1.52 m^3/m/year). A total volume of ~2,100,000 m^3 (3.0 m^3/m/year) of sand was eroded from the shoreface and beach over the same period of observation. Thus, overwash processes account for a little over half of the sand produced by shoreline erosion in historical time. The other half is likely being transported farther west via alongshore transport (Wallace et al. 2010) and spread out in the shoreface and downdrift beaches. The barrier is estimated to have translated landwards to the present location at a rate of 0.17–0.27 m/year during the past 3 ka, which is an order of magnitude slower than the current rate.

The back-barrier accommodation is 40,500,000 m^3 (the areal extent of Christmas Bay is ~27,000,000 m^2 and water depth averages 1.5 m). The volume of sand in Follets Island is ~14,000,000 m^3 (5,500,000 m^3 sand for the barrier and 8,500,000 m^3 sand in the back-barrier). Thus, back-barrier accommodation is about three times greater than the volume of sand in Follets Island.

Back-barrier morphology, vegetation, and substrate slope also control overwash rates. Barrier islands with low-gradient substrates and back-barrier accommodation space migrate rapidly (Swift and Moslow 1982; Pilkey and Davis 1987; Cowell et al. 2003; Storms and Swift 2003; Stolper et al. 2005; Donnelly et al. 2006; FitzGerald et al. 2008; Moore et al. 2010; Brenner et al. 2015). Overwash is removing and transporting half of the available sand landwards from the undernourished barrier. Therefore, this depletion will likely cause barrier over-stepping (negative sediment budget) during sea-level rise (Cowell et al. 1995; Stolper et al. 2005).

Because only about half of the eroded shoreline sand is deposited as overwash, the barrier is getting lower and narrower, which will likely lead to increases in overwash flux in the future (Schwartz 1975; Cowell et al. 2003; Stolper et al. 2005; Rosati et al. 2006; FitzGerald et al. 2008; Park and Edge 2011). Low-gradient, narrow barrier islands are prone to overwash and therefore to multiple breaches, especially during accelerated sea-level rise, potentially leading to barrier disintegration and break up (such as identified for pre-historical time along the North Carolina Outer Banks by Mallinson et al. this volume). Given that accommodation of Christmas Bay greatly exceeds sand available in the barrier island system and that sand supply rates are diminished, the island will likely transition from a subaerial barrier to subaqueous shoals in the foreseeable future, similar to environments like

Table 2 Input parameter
values used in Fig. 12

Parameter	Units	Value
Maximum overwash flux	m³/m/year	10, 20, 30
Shoreface response rate	m³/m/year	5,000
Equilibrium shoreface slope	–	0.02
Shoreface toe depth	m	10
Equilibrium island width	m	400
Equilibrium island height	m	2
Back-barrier lagoon slope	m	10^{-4}
Sea-level rise rate	mm/year	0–10

the Chandeleur Islands and the central Mexico coast. Extrapolating the historical fluxes of overwash and shoreline erosion rates, we estimate that Follets Island will likely drown in ~260 years (see Sect. 4.3.2). This estimate, however, does not account for the effect of accelerated sea-level rise and barrier narrowing.

Storm frequency along the Texas coast does not appear to have increased in historical time relative to the late Holocene (Wallace and Anderson 2010), although stronger but fewer storms are projected globally by the end of the century (Lin et al. 2012; Woodruff et al. 2013). Storms dominate shoreface erosion, but the interplay between sea-level rise and sediment supply is the main driver of the long-term rate of shoreline retreat (Woodruff et al. 2013). Therefore, storms are not the sole cause of increased erosion and washover of Follets Island.

Most of the barriers of the Texas Coast were formed less than 5000 years ago when the sea-level rise rate in the northern Gulf of Mexico region decreased from an average rate of 1.4 mm/year to about 0.4–0.6 mm/year (Milliken et al. 2008; Anderson et al. 2014). Current sea-level rise in the region is estimated to be ~3.0 mm/year (NOAA 2015), or about five times the rate when most Texas barriers were formed. This does not account for subsidence, which depends on rates of compaction of Holocene sediments (Törnqvist et al. 2008), and more than double sea-level rise rates locally.

Field observations from Rodriguez et al. (this volume) suggest an abrupt increase in the rate of sea-level rise makes barrier islands vulnerable to overwash leading to reductions in the width and height of a barrier and increasing the rate of shoreline retreat. Additionally, recent modeling efforts (Moore et al. 2010; Lorenzo-Trueba and Ashton 2014; Cowell and Kinsela this volume; Murray and Moore this volume; Ashton and Lorenzo-Trueba this volume) emphasize the sensitivity of barrier island response to sea-level rise. In particular, using generic island characteristics similar to those used by Lorenzo-Trueba and Ashton (2014) (see Table 2), we find that a change in sea-level rise rate from 1 to 10 mm/year can result in a 4-fold increase in the magnitude of shoreline retreat within a 100-year time period (Fig. 12). This result does not depend on the maximum overwash flux used as an input in the model. Although more analysis is needed, we suggest that the acceleration in sea-level rise
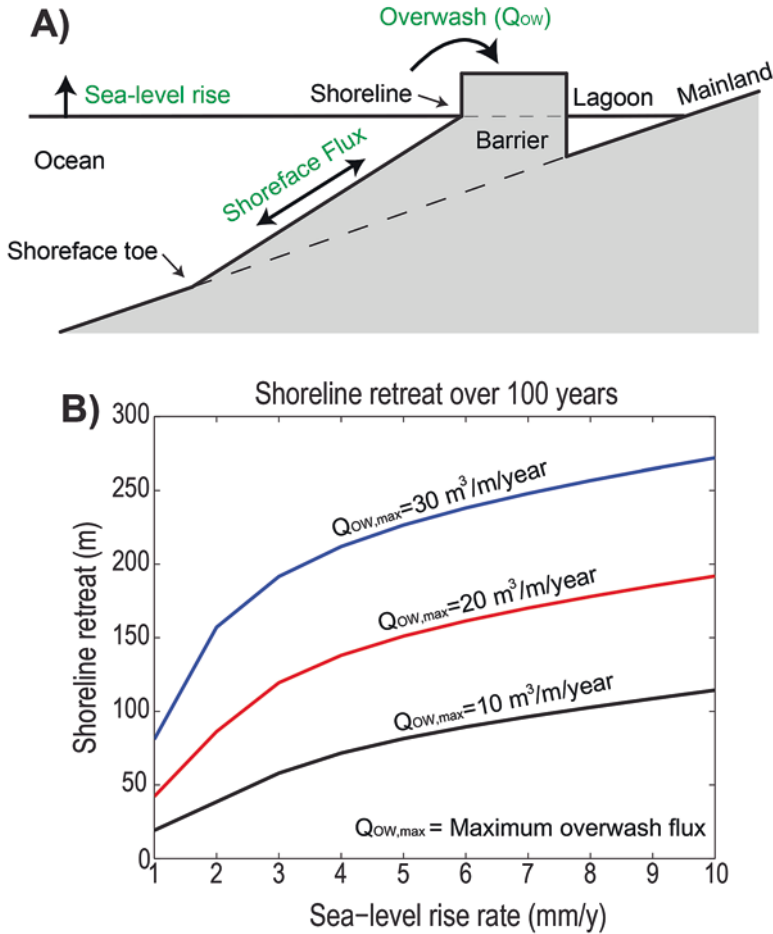
Fig. 12 (**a**) Barrier model setup and components (Lorenzo-Trueba and Ashton 2014). Note the strong exaggeration of the vertical scale. (**b**) Shoreline retreat during barrier landward migration as a function of the sea-level rise rate. Input parameter values are included in Table 2

has played a significant role on the unprecedented rate of shoreline erosion of Follets Island.

Diminished sand supply is likely also contributing to the unprecedented erosion on Follets Island. Sand supply from the east is regulated by dynamic processes operating within the San Luis Pass tidal inlet/delta complex, and sand rarely discharges from the inlet towards Follets (Wallace and Anderson 2013). The east end of Follets Island has experienced significant erosion during historical time (Fig. 2a) and this sand is moving west (Wallace et al. 2010). In addition, diversion of the Brazos River mouth from its pre-1929 location at Surfside Beach and construction of jetties at the former river mouth (at the west end of Follets Island) have blocked sand delivery from the west (Morton and Pieper 1975) (Fig. 1). The State of Texas

has undertaken several beach nourishment projects at Surfside Beach in recent decades only to have nourishment sands disappear within months of when these projects where completed.

Follets Island could transition from a rollover subaerial barrier to subaqueous shoals within the next few centuries. Exactly when this will happen depends on the number and magnitude of storms that will impact the island during this time. Regardless, the role of the island as a natural barrier to storm impact on inland areas will significantly diminish. Our volume and flux estimates indicate that sustaining the island by beach nourishment would require volumes of sand that currently do not exist in the nearshore zone as little sand exists seaward of the upper shoreface to a distance of approximately 40 km offshore (Anderson et al. 2014). Given the paucity of sand available to Follets Island and high rates of overwash, sand nourishment would have to come from sources on the continental shelf that are far removed from the island.

6   Conclusions

Follets Island is the thinnest barrier island and one of the fastest retreating islands on the Texas coast. Landward translation of the island is manifest as a surface of erosion, ~1.5 m deep, which is a sharp, planar surface that separates back-barrier deposits from overlying shoreface-foreshore deposits. Our results show that current shoreline erosion rates for Follets Island are unprecedented, with current rates being as much as an order of magnitude faster than the long-term (millennial) rate. This increase was associated with an increase in sand overwash rates over historic relative to geologic time.

Results show that the washover flux for the island accounts for at least half the volume of sand produced by shoreline erosion. Accelerated sea-level rise and diminished sand supply are considered the key causes of unprecedented shoreline erosion of the barrier.

At the current rate of shoreline retreat and overwash, coupled with the diminished sand supply and large back-barrier accommodation of Christmas Bay, Follets Island could transition from a rollover subaerial barrier to subaqueous shoals in the next few centuries. Its role as a barrier to storm impact is being significantly diminished. Barriers similarly impacted by accelerated sea-level rise and reduced sand supply could suffer the same fate.

References

Anderson J, Milliken K, Wallace D et al (2010) Coastal impact underestimated from rapid sea level rise. EOS Trans Am Geophys Union 91:205–206

Anderson JB, Wallace DJ, Simms AR et al (2014) Variable response of coastal environments of the northwestern Gulf of Mexico to sea-level rise and climate change: implications for future change. Mar Geol 352:348–366

Appleby PG (1998) Dating recent sediments by 210Pb: problems and solutions. In: Dating of sediments and determination rate, vol. STUK-A145, Helsinki, pp 7–24

Appleby PG, Oldfield F (1983) The assessment of 210Pb data from sites with varying sediment accumulation rates. Hydrobiologia 103:29–35

Ashton AD, Lorenzo-Trueba J (2018) Morphodynamics of barrier response to sea-level rise. In: Moore LJ, Murray AB (eds) Barrier dynamics and response to changing climate. Springer, New York

Bernard HA, Major CF Jr, Parrot BS (1959) The Galveston Barrier Island and environments: a model for predicting reservoir occurrence and trend. Trans Gulf Coast Assoc Geol Soc 9:221–224

Bernard HA, Major CF Jr, Parrot BS et al (1970) Recent sediments of Southeast Texas: a field guide to the Brazos alluvial and deltaic plains and the Galveston barrier island complex. University of Texas, Bureau of Economic Geology Guidebook 11, Austin, TX, p 132

Boyd R, Penland S (1984) Shoreface translation and the Holocene stratigraphic record: examples from Nova Scotia, the Mississippi Delta and eastern Australia. Mar Geol 60:391–412

Brenner OT, Moore LJ, Murray AB (2015) The complex influences of back-barrier deposition, substrate slope and underlying stratigraphy in barrier island response to sea-level rise: insights from the Virginia Barrier Islands, Mid-Atlantic Bight, U.S.A. Geomorphology 246:334–350

Bruun P (1954) Coastal erosion and development of beach profiles. Tech. Rep. Memo 44, U.S. Army Corps of Eng., Vicksburg, MS

Bruun P (1962) Sea-level rise as a cause of shore erosion. J Waterway Harbor Coast Eng Div 88:117–132

Carlin J, Dellapenna T, Figlus J et al (2015) Investigating morphological and stratigraphic changes to the submarine shoreface of a transgressive Barrier Island: Follets Island, Northern Gulf of Mexico. In: Wang P, Rosati JD, Cheng J (eds) Coastal sediments: the proceedings of the coastal sediments 2015. World Scientific, Singapore

Carruthers EA, Lane PD, Evans RL et al (2013) Quantifying overwash flux in barrier systems: an example from Martha's Vineyard, Massachusetts, USA. Mar Geol 343:15–28

Cowell PJ, Kinsela MA (2018) Shoreface controls on barrier evolution and shoreline change. In: Moore LJ, Murray AB (eds) Barrier dynamics and response to changing climate. Springer, New York

Cowell PJ, Roy PS, Jones RA (1995) Simulation of large-scale coastal change using a morphological behaviour model. Mar Geol 126:45–61

Cowell PJ, Stive MJF, Niedoroda AW et al (2003) The coastal-tract (part 2): applications of aggregated modeling of lower-order coastal change. J Coast Res 19:828–848

Dean RG, Maurmeyer EM (1983) Models for beach profile response. CRC handbook of coastal processes and erosion. CRC Press, Boca Raton, pp 151–165

Donnelly C, Kraus N, Larson M (2006) State of knowledge on measurement and modeling of coastal overwash. J Coast Res 22:965–991

Faure G (1986) Principles of isotope geology. Wiley, New York, p 589

FitzGerald DM, Fenster MS, Argow BA et al (2008) Coastal impacts due to sea-level rise. Annu Rev Earth Planet Sci 36:601–647

FitzGerald DM, Hein C, Hughes Z, Kulp M, Georgiou I, Miner M (2018) Runaway barrier island transgression concept: global case studies. In: Moore LJ, Murray AB (eds) Barrier dynamics and response to changing climate. Springer, New York

Gibeaut JC, White WA, Hepner T et al (2000) Texas Shoreline Change Project: Gulf of Mexico shoreline change from the Brazos River to Pass Cavallo. Bureau of Economic Geology, The University of Texas at Austin, Report to the Texas Coastal Coordination Council and the General Land Office, contract no. NA870Z0251, p 32

Harter C, Figlus J, Dellapenna T (2015) The role of hurricanes on the morphological evolution of a sediment-starved barrier island along the upper Texas coast: Follets Island. In: Wang P, Rosati JD, Cheng J (eds) Coastal sediments: the proceedings of the coastal sediments 2015. World Scientific, Singapore

Inman DL, Dolan R (1989) The Outer Banks of North Carolina: budget of sediment and inlet dynamics along a migrating barrier system. J Coast Res 5(2):193–237

Leatherman SP (1983) Shoreline mapping: a comparison of techniques. Shore Beach 7:28–33

Lin N, Emanuel K, Oppenheimer M et al (2012) Physically based assessment of hurricane surge threat under climate change. Nat Clim Chang 2(6):462–467

Lorenzo-Trueba J, Ashton AD (2014) Rollover, drowning, and discontinuous retreat: distinct modes of barrier response to sea-level rise arising from a simple morphodynamic model. J Geophys Res Earth 119:779–801

Mallinson D, Culver S, Leorri E, Mitra S, Mulligan R, Riggs S (2018) Barrier Island and estuary co-evolution in response to Holocene climate and sea-level change: Pamlico Sound and the Outer Banks Barrier Islands, North Carolina, USA. In: Moore LJ, Murray AB (eds) Barrier dynamics and response to changing climate. Springer, New York

McBride RA, Byrnes MR (1997) Regional variations in shore response along barrier island systems of the Mississippi River delta plain: historical change and future prediction. J Coast Res 13:628–655

Milliken KT, Anderson JB, Rodriguez AB (2008) A new composite Holocene sea-level curve for the northern Gulf of Mexico. In: Anderson JB, Rodriguez AB (eds) Response of Upper Gulf Coast Estuaries to Holocene climate change and sea-level rise. Geological Society of America Special Paper 443, pp 1–11

Moore LJ, List JH, Williams SJ et al (2010) Complexities in barrier island response to sea level rise: insights from numerical model experiments, North Carolina Outer Banks. J Geophys Res 115:F03004. https://doi.org/10.1029/2009JF001299

Moore LJ, Patsch K, List JH et al (2014) The potential for sea-level-rise-induced barrier island loss: insights from the Chandeleur Islands, Louisiana, USA. Mar Geol 355:244–259

Morton RA (1994) Texas barriers. In: Davis RA (ed) Geology of Holocene barrier island systems. Springer, New York, pp 75–114

Morton RA, Amdurer M (1974) Environmental geology in coastal zone development: an analysis of physical properties and processes. University of Texas, Bureau of Economic Geology, Austin, p 103

Morton RA, Paine J G (1985) Beach and vegetation-line changes at Galveston Island, Texas: erosion, deposition, and recovery from Hurricane Alicia. The University of Texas at Austin, Bureau of Economic Geology, Geological Circular 85-5, p 39

Morton RA, Pieper MJ (1975) Shoreline changes on Brazos Island and South Padre Island (Mansfield Channel to mouth of the Rio Grande). The University of Texas at Austin, Bureau of Economic Geology Geological Circular 75-2, p 39

Morton RA, Sallenger AH (2003) Morphological impacts of extreme storms on sandy beaches and barriers. J Coast Res 19:560–573

Morton RA, Gibeaut JC, Paine JG (1995) Meso-scale transfer of sand during and after storms: implications for prediction of shoreline movement. Mar Geol 126:161–179

Morton RA, Miller TL, Moore LJ (2004) National assessment of shoreline change: part 1: historical shoreline changes and associated coastal land loss along the U.S. Gulf of Mexico. U.S. Geological Survey Open-file Report 2004-1043, p 45

National Oceanic and Atmospheric Administration (2015) Tides and Currents. http://tidesandcurrents.noaa.gov. Accessed 4 Jul 2015

Murray AB, Moore LJ (2018) Geometric constraints on long-term barrier migration: from simple to surprising. In: Moore LJ, Murray AB (eds) Barrier dynamics and response to changing climate. Springer, New York

Niedoroda AW, Swift DJP, Figueiredo AG et al (1985) Barrier island evolution, middle Atlantic shelf, USA Part 2: evidence from the shelf floor. Mar Geol 63(1–4):363–396

Paine JG (1993) Subsidence of the Texas coast: inferences from historical and late Pleistocene sea levels. Tectonophysics 222:445–458

Paine JG, Sojan M, Tiffany C (2012) Historical shoreline change through 2007, Texas Gulf Coast: Rates, contributing causes, and Holocene context. Gulf Coast Assoc Geol Soc J 1:13–26

Paine JG, Caudie TL, Andrews JR (2017) Shoreline and sand storage dynamics from annual airborne LIDAR surveys, Texas Gulf coast. J Coast Res 33(3):487–506

Park YH, Edge BL (2011) Beach erosion along the northeast Texas coast. J Coast Res 27:502–514

Pilkey OH, Davis, TW (1987) An analysis of coastal recession models: North Carolina coast. Society of Economic and Paleontologists and Mineralogists, pp 59–68

Reimer PJ, Bard E, Bayliss A et al (2013) IntCal13 and Marine13 radiocarbon age calibration curves 0–50,000 years cal BP. Radiocarbon 55:1869–1887

Rodriguez AB, Fassell ML, Anderson JB (2001) Variations in shoreface progradation and ravinement along the Texas coast, Gulf of Mexico. Sedimentology 48:837–853

Rodriguez AB, Anderson JB, Siringan FP et al (2004) Holocene evolution of the east Texas coast and inner continental shelf: along strike variability in coastal retreat rates. J Sediment Res 74:405–421

Rodriguez AB, Yu W, Theuerkauf EJ (2018) Abrupt increase in washover deposition along a transgressive barrier island during the late 19th century acceleration in sea-level rise. In: Moore LJ, Murray AB (eds) Barrier dynamics and response to changing climate. Springer, New York

Rosati JD, Stone GW, Dean RG et al (2006) Restoration of barrier islands overlying poorly -consolidated sediments, south-central Louisiana. Gulf Coast Assoc Geol Soc Trans 56:727–740

Schwartz RK (1975) Nature and genesis of some storm washover deposits. U.S. Army Corps of Engineers, Coastal Engineering Research Center Technical Memorandum No. 61, p 69

Simms AB, Anderson JB, Blum M (2006) Barrier-island aggradation via inlet migration: Mustang Island, Texas. Sediment Geol 187:105–125

Siringan FP, Anderson JB (1994) Modern shoreface and inner-shelf storm deposits off the East Texas coast, Gulf of Mexico. J Sediment Res 64:99–110

Stéphan P, Suanez S, Fichaut B (2012) Long-term morphodynamic evolution of the Sillon de Talbert gravel barrier (Brittany, France). Shore Beach 80(1):19–36

Stive MJF, de Vriend HJ (1995) Modelling shoreface profile evolution. Mar Geol 126:235–248

Stolper D, List JH, Thieler ER (2005) Simulating the evolution of coastal morphology and stratigraphy with a new morphological-behaviour model (GEOMBEST). Mar Geol 218(1):17–36

Storms JEA, Swift DJP (2003) Shallow-marine sequences as the building blocks of stratigraphy: Insights from numerical modelling. Basin Res 15(3):287–303

Swift DJP (1976) Continental shelf sedimentation. In: Stanley DJ, Swift DJP (eds) Marine sediment transport and environmental management. Wiley, New York, pp 311–350

Swift DJP, Moslow TF (1982) Holocene transgression in South-Central Long Island, New York: discussion. J Sediment Res 52(3):1014–1019

Swift DJP, Niedoroda AW, Vincent CE et al (1985) Barrier island evolution, Middle Atlantic Shelf U.S.A., part 1: shoreface dynamics. Mar Geol 63:331–361

Taha ZP, Anderson JB (2008) The influence of valley aggradation and listric normal faulting on styles of river avulsion: a case study of the Brazos River, Texas, USA. Geomorphology 95:429–448

Thieler ER, Pilkey OH, Young RS et al (2000) The use of mathematical models to predict beach behavior for US coastal engineering: a critical review. J Coast Res 16:48–70

Törnqvist TE, Wallace DJ, Storms JEA et al (2008) Mississippi Delta subsidence primarily caused by compaction of Holocene Strata. Nat Geosci 1:173–176

Wallace DJ, Anderson JB (2010) Evidence of similar probability of intense hurricane strikes for the Gulf of Mexico over the late Holocene. Geology 38:511–514

Wallace DJ, Anderson JB (2013) Unprecedented erosion of the upper Texas Coast: response to accelerated sea-level rise and hurricane impacts. Geol Soc Am Bull 125:728–740

Wallace DJ, Anderson JB, Rodriguez AB (2009) Natural versus anthropogenic mechanisms of erosion along the upper Texas coast. In: Kelley JT, Pilkey OH, Cooper JAG (eds) America's most vulnerable coastal communities. Geological Society of America Special Paper 460, pp 137–147

Wallace DJ, Anderson JB, Fernández RA (2010) Transgressive ravinement versus depth of closure: a geological perspective from the upper Texas coast. J Coast Res 26:1057–1067

Wilkinson BH (1975) Matagorda Island, Texas: the evolution of a Gulf coast barrier complex. Geol Soc Am Bull 86:959–967

Wilkinson BH, Basse RA (1978) Late Holocene history of the central Texas coast from Galveston Island to Pass Cavallo. Geol Soc Am Bull 89:1592–1600

Woodruff JD, Irish JL, Camargo SJ (2013) Coastal flooding by tropical cyclones and sea-level rise. Nature 504(7478):44–52